

Article ID: 1000-8152(2008)01-0125-08

新能源发电中控制及电力电子技术专题

编者按:由华南理工大学、香港理工大学、台湾成功大学、广东省电机工程学会风电专委会以及广东省技术经济研究发展中心发起,由我刊等单位承办的“新能源发电中的控制与电力电子技术”学术交流会已于2007年11月26~29日在广州-汕头举行。会议收到论文40余篇,集中展示了我国在新能源领域控制与电力电子技术方面的研究现状与成果。为推动和促进上述技术的发展与应用,本刊在《控制理论与应用》2008年第1期以及2008年第2期刊登“新能源发电中的控制与电力电子技术”的部分文章,以期达到加强宣传与扩大影响的效果。

《控制理论与应用》编辑部

Switched mode power conversion for alternative energy

CHENG K.W. Eric

(Power Electronics Research Center, Department of Electrical Engineering, The Hong Kong Polytechnic University,
Hung Hom, Hong Kong, China)

Abstract: The solar power conditioning and the wind power conditioning systems are discussed in this paper. Various maximum power point tracking methods are examined. The power electronic converter topologies for power point tracking and voltage conversion are studied in this paper. Other power conditioning systems are also studied, including the inverter drives, battery charger and DC-DC and AC-AC power converters. This paper gives an overview of the recent development of the power converters and drive circuits in the area. Concentration has been put on different maximum power point tracking methods, and brief description of each type is shown.

Key words: switched mode power conversion; maximum power point tracking; alternative energy

新能源发电系统中的电力电子变换器

郑家伟

(香港理工大学 电机工程系 电力电子研究中心, 香港 红勘)

摘要:讨论了太阳能发电和风力发电的条件及其适应器,并且对各种最大功率点跟踪方法进行验证。论文研究了电力电子变换器拓扑技术在最大功率点跟踪及电压变换方面的应用。另外,发电系统还包括:逆变器驱动电路,蓄电池充电器,DC-DC和AC-AC电力变换器。本文对新能源领域中电力变换器及其驱动电路的最新发展做了全面的综述;其中,重点介绍了所用到的不同的最大功率跟踪方法并给用到的各种类型进行简单描述。

关键词: 电力电子变换器; 最大功率点追踪; 新能源

中图分类号: TM46 文献标识码: A

1 Introduction

All the alternative energy sources have power processing stage for power conditioning. The power conditioning provides voltage, current or impedance trans-

formation for matching the source and load. The source can be in AC or DC that depends on the alternative energy source. The power processing units are to convert the AC or DC into suitable voltage for load or interme-

Received 20 July 2007; revised 23 October 2007.

This work described in this paper was fully supported by the Power Electronics Research Center and the Research Office of the Hong Kong Polytechnic University, Hong Kong, China.

diate power stage.

Alternative energy sources such as photovoltaic (PV) system and fuel cells are DC source. The voltage output is not a constant and depends on the energy input and the loading. For photovoltaic systems, the output voltage depends on the illumination level to the cell and loading current. Therefore a power conditioning unit is designed with maximum power-point tracking (MPT) in order to optimize the efficiency^[1,2]. The fuel cell voltage depends on the input fuel concentration and rate^[3], and the loading. A maximum power tracking is also needed.

For the electromagnetic machine types of alternative source, it is usually the induction generator, synchronous generator or switched-reluctance generator. The output voltage is AC and is needed to be regulated. Some generators also require a PWM driver to maintain the operating point in a certain frequency range for power optimization and frequency control. The output stage of the generator requires an AC-DC conversion for voltage regulation or AC-AC conversion for both voltage and frequency regulation. The AC-DC converters are usually bridge types of topologies. The power factor is needed to be controlled so that the generator will be working with a higher power factor near 1 in order to optimize the efficiency of the machines.

The power processing stage is of high power, and the switched mode power conversion topologies employs high power converter such as bridge converter. They can provide bidirectional power flow^[4], resonant switching or soft-switching, and multiple output voltage. The grid connected DC-AC power conversion is also very popular for second stage power conversion which processes the intermediate power stage supplying a DC to other load. In this paper, the power conversion unit is discussed. Suitable topology is examined for the use in alternative energy sources.

2 Photovoltaic maximum power point tracking

A. Analytic tuning

The classical method of maximum power-point tracking is usually based on iteration. It may give unstable tracking and oscillate around some operation point. Ref[5] derives a tangential method such that the MPT can be defined by a tangent to the line joining the x -intercept and y -intercept of the $i - v$ characteristic of the solar cell. Fig.1 shows a typical $i_p - v_p$ charac-

teristic of a solar cell. The maximum power is a line tangential to the $x - y$ intercept line as shown.

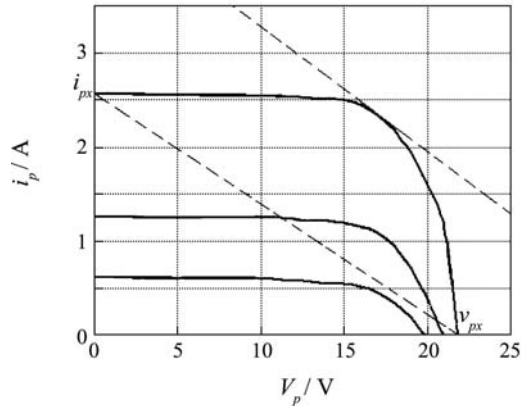


Fig. 1 Current-voltage MPT characteristics of photovoltaic cell

If i_{px} is the y -intercept of i_p on the y -axis and v_{px} is the x intercept of v_p on the x -axis. The slope of the tangent is

$$S_x = -\frac{i_{px}}{v_{px}}. \quad (1)$$

At the maximum power point, the maximum power P_m :

$$\frac{di_p}{dv_p} \Big|_{P_m} = S_x. \quad (2)$$

The duty ratio control of the DC-DC converter is adjusted to regulate the same slope as S_x for achieving MPT.

B. Switching frequency modulation

The maximum power transfer from photovoltaic panel to DC-DC power converter is governed by the fundamental equations^[6]:

$$R_s = R_i, \quad (3)$$

where R_s is the source resistance and R_i is the DC-DC converter input resistance. The load resistance R of the DC-DC power converter can be expressed as

$$R_i = \frac{R}{M^2}, \quad (4)$$

where M is the voltage conversion ratio. M depends on duty ratio d for continuous mode, load resistance R , converter inductance L and operating frequency f_s :

$$M = f(d, R, L, f_s). \quad (5)$$

For continuous inductor conduction mode:

$$M = f(d). \quad (6)$$

The duty ratio of the DC-DC converter can be ex-

pressed as:

$$R_s = \frac{R}{f^2(d_M, R, L, f_s)}, \quad (7)$$

where d_M is the value of d when MPT is achieved. Ref[6] suggests that the MPT relationship can be developed by using the error signal:

$$e(\alpha) = \phi \frac{1 - \alpha^2}{(1 + \alpha^2)^2}, \quad (8)$$

where

$$\alpha = \frac{d}{d_M} \quad (9)$$

and

$$\phi = \hat{f}_s / (2f_s), \quad (10)$$

\hat{f}_s is a smaller modulation signal which is added to the switching frequency signal. The duty ratio is ruled by

$$\text{sgn}(d - d_M) = -\text{sgn}(e(\alpha)). \quad (11)$$

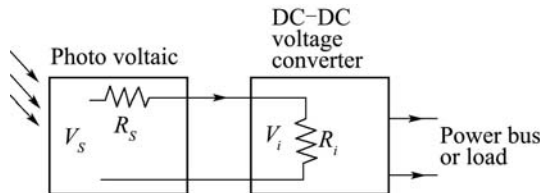


Fig. 2 The maximum power transfer illustration

C. $p-n$ junction diode equivalent tracking

The $p-n$ junction forward characteristic of a diode is very close to the solar cell. The voltage drop of the diodes can be used as a reference voltage to track the maximum power^[7]. Fig.3 shows the schematic diagram.

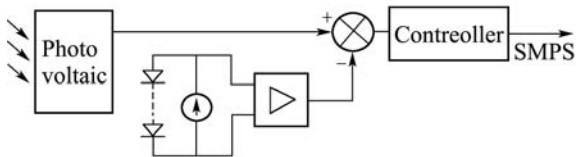


Fig. 3 $p-n$ junction equivalent method to detect the MPT

The diodes used for the comparison is attached to the photovoltaic panel so that both the photovoltaic and the diodes experience the same temperature environment^[8].

D. Slope detection for fast MPT

Conventional method also uses the sign of slope

$$S_p = \frac{dP_p}{dv_p}, \quad (12)$$

to obtain the MPT that may not achieve fast or accurate power tracking. Fig.4 shows the power P_p against v_p .

A fast MPT^[9] integrates the slope with time to obtain a fast tracking method. As it can be seen from Fig.4, when the instantaneous tracking point is away from the maximum, the slope integration will increase to accelerate the response to approach the maximum power point.

$$d = k_e e = k_p \int S_p dt, \quad (13)$$

where k_e and k_p are constant.

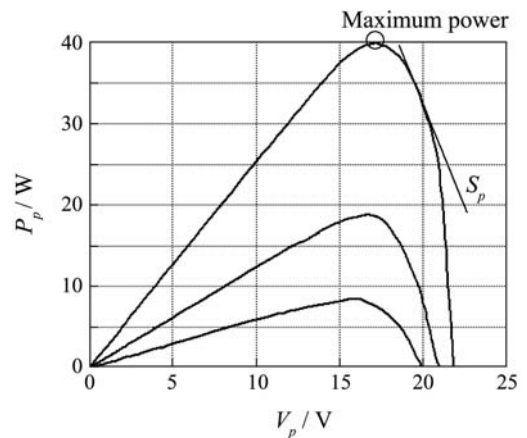


Fig. 4 Fast maximum power point tracking

3 DC-DC power conversion

The DC-DC power conversion is a typical unit in the alternative energy system. It provides voltage conversion or impedance conversion. The single-ended power converter is employed for low power applications and renewable energy system. Besides, the typical switched mode power supply (SMPS) topologies are Buck, Boost and Buck-boost^[4]. The following will discuss different new topologies for the applications.

A. Non isolated and isolated SMPS

For low power applications and non isolation cases, a single transistor can be used. The voltage conversion ratio M for continuous inductor L conduction mode is also shown. For information, M for common circuits Buck, Boost and Buck-boost, Cuk, Sepic and Zeta are d , $1/(1-d)$ and $d/(1-d)$, $d/(1-d)$, $d/(1-d)$ and $d/(1-d)$, respectively. For a wide range of voltage conversion ratio or a DC isolation is needed, the transformer isolated version can be used. The output stage must be isolated from the PV through transformer. For information, M for common circuits Forward and Fly-back are dN_2/N_1 and $dN_2/((1-d)N_1)$.

B. Phase angle control

The bridge converter for phase control^[4] is to control the phase shift δ between the two legs. The volt-

age conversion ratio is $M = \delta N_2 / (\pi N_1)$. For maximum phase shift, $\delta = \pi$. The H-bridge converter is the most suitable one for high power applications. They also have the additional advantage of soft-switching, i.e., zero-voltage switching.

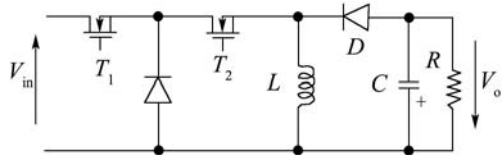


Fig. 5 Buck-Buck-Boost phase converter,
 $M = (D_1 - \delta) / (1 - D_2)$

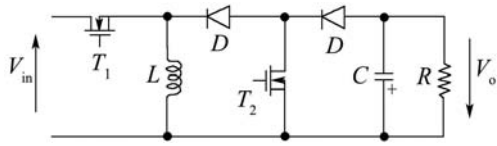


Fig. 6 Buck-Boost-BB phase converter,
 $M = D_1 / (1 - D_2 - \delta)$

Fig.5 and Fig.6 show two versions of the buck-boost phase converters, the Buck-Boost-Boost phase converter and the Buck-Boost-BB phase converter, respectively. Both circuits can regulate the duty ratios D_1 and D_2 of the transistors T_1 and T_2 , respectively. It can also be controlled by the phase angle δ between the two transistors. The above topologies give additional control capability for photovoltaic panel and users can select the converter according to the criteria of voltage conversion ratio, output voltage inverted or non-inverted, transformer isolated and continuous input current for input or output. It allows higher conversion capability than simple buck or boost converter and is suitable for alternative energy source which may have a very wide range of output voltage and power.

4 System topologies

A. Battery system

Photovoltaic system can be used independently for supplying power to load or be connected to the grid. The former requires battery storage which provides immediate energy storage^[10]. When solar energy is not sufficient, the charged battery supplies power to the load as shown in Fig.7. The circuit requires sufficient number of battery storages and a good battery charger. Other energy storages are also available such as hydrogen energy storage, etc.

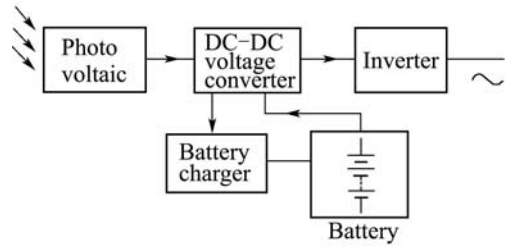


Fig. 7 PV system with typical power processing

B. Energy storage

Besides the battery storage, the hydrogen storage has been using recently^[11]. Fig.8 shows the schematic diagram. The system is usually combined with the fuel cell. The power from the alternative energy source is not stored in battery but through electrolyzer in which decomposes the water into oxygen and hydrogen. The hydrogen is stored in the compressed high pressure storage tank and can be transported to other locations. It can also be transported through gas pipe. The hydrogen is then converted to water through the fuel cell. The best efficiency of electrolyzer is around 85%^[12]. The fuel cell efficiency is around 35%^[13]. The best is around 40~50%^[14]. The combined efficiency is expected to be 30%. Comparison of efficiencies for input to output power conversion is shown in Table 1^[15]. Obviously, the efficiency of the battery storage is higher than the hydrogen energy storage. The energy density of a hydrogen tank is higher. For a low pressure tank, 170 Wh/kg can be achieved. For some commercial tank, Millennium Cell's hydrogen storage^[16] can reach 425 Wh/kg.

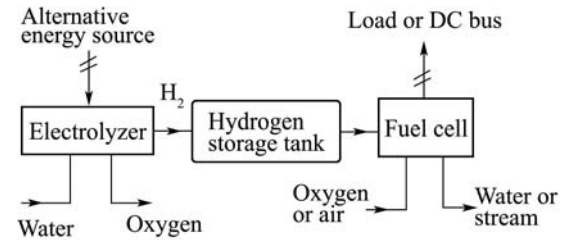


Fig. 8 Energy storage system with hydrogen

Table 1 Comparison of different batteries

Type	Cell voltage/V	Density/(Wh·kg)	Efficiency/%
<i>Lead-acid</i>	2.1, 2.2	30~40	70~95
<i>Ni-Cad</i>	1.2	40~60	70~90
<i>Ni-iron</i>	1.2	50	65
<i>NiMH</i>	1.2	30~80	66
<i>Li-ion Monomer</i>	3.6	160	99
<i>Nano Titanate</i>	13.8	90	87~95

Supercapacitor is also considered for energy stor-

age. Any voltage or capacitance can be made by different combinations. They are not used for high energy storage^[17] but used for assistive energy storage. The dynamic response for the supercapacitors is better than batteries; therefore they are used in parallel with the battery to improve the dynamic performance. A typical example is the electric vehicle.

C. Grid connected system

The energy storage in the battery can be inverted to the grid for reducing the number of the batteries. Some systems are directly connected to grid. Fig.9 shows the connection of the PV system to a DC bus. The DC bus is connected by a number of PV panels which is connected in series or parallel. The load in the DC bus can also be shared in a suitable manner so that MPT of the DC-DC voltage converter can be achieved.

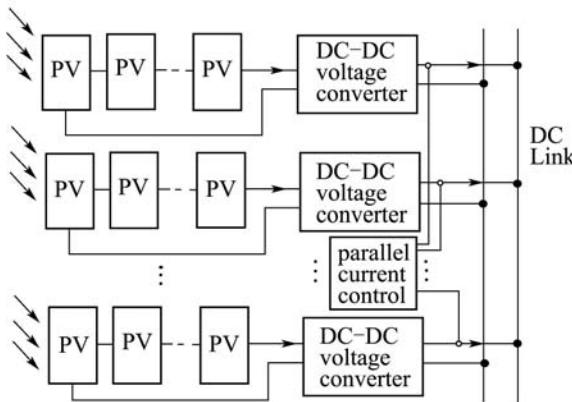


Fig. 9 Parallel sharing of PV systems

The DC bus link can be inverted to AC for loading or connected to grid as shown in figure. The output voltage V_{AC} from the inverter is 380 V or the local mains voltage. The inverter equation is:

$$V_{DC} = \frac{2\sqrt{2}V_{AC}}{M}, \quad (14)$$

where M is the modulation index and can be varied from 0.4 to 1.15. Too small M gives poor harmonic spectrum that is to be avoided. The typical value is 0.9.

5 Battery charger

The battery charger provides a number of stages of charging mechanism, including constant voltage, constant current, trickle and/or pulse charging. The battery charging circuit employs the bidirectional power flow transistor topologies and provides bi-directional power flow between the battery and the load circuit.

A. Circuit topology

The following shows a typical list of the circuit

topology for the battery charger. If M is the charging conversion and $1/M$ is the conversion ratio for discharging, In some applications, the charging and discharging employ separate circuits if the input source V_{in} is not the DC link, a separate DC-DC converter is used to connect the battery to the load and the charger circuit. Fig.10 shows a typical charging circuit.

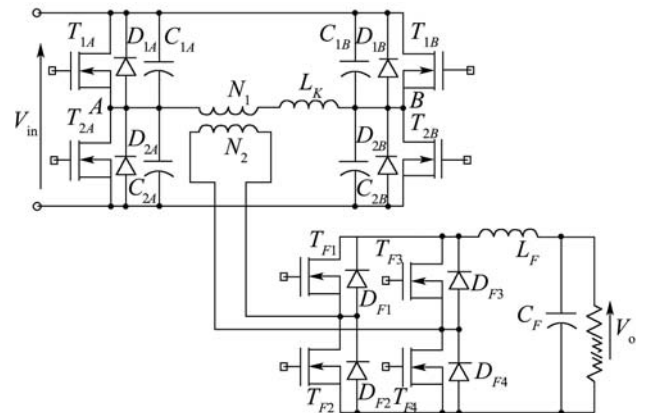


Fig. 10 Charger topologies: H-bridge, $M = \delta N_2 / (\pi N_1)$

B. Comment on topologies

The Buck version is a popular circuit which can provide step down from PV array or main DC-DC converter to the battery. Choke L is used to reduce the ripple. T_1 and T_2 are responsible for the main and auxiliary transistors, respectively. T_1 is for delivering the energy from the input side to the battery whereas T_2 is to feed the battery energy back to the V_{in} stage. The Boost version is to boost up the V_{in} to higher voltage. The current ripple of the input stage is particularly low. It is suitable for low electromagnetic interference (EMI) applications. Both the Buck-Boost version and the Cuk version can provide a wide range of battery voltage. The voltage conversion can be step-up or step-down that depends on the transistor duty ratio d . The Cuk version has the additional advantage of low ripple in both output voltage and input current, but the drawback is that it has larger number of components. The above four examples provide voltage conversion from order 1 to 3 of magnitude. For higher magnitude of voltage conversion, a transformer isolation version should be used^[4].

C. Isolated version

The bi-directional power flow version can be done by changing the diode to transistor. For the Forward conversion, the D_1 and D_2 are needed to change to transistor. This circuit is so called the isolated-boost^[4] and has more transistors than the other circuit therefore it is not economic. The bi-directional version of the flyback

conversion is just to change diode to transistor. It is the same voltage conversion ratio viewed from either end. M is inverted with d changed to $1 - d$.

6 Inverter topology

For 3-phase version, it is basically a full-bridge version with 3 inverter legs (3 pairs of transistors). The inverter is fired by PWM signals and produces sinusoidal output voltage. The inverter output should be filtered to remove the high frequency switching signal. The input voltage V_{DC} to the inverter is related to the output voltage V_{AC} by (14).

7 VFCF converter

Fig.11 shows the popular schematic diagram of the generators for wind power, including doubly-fed generator^[18], synchronous generator^[19] or induction generator^[20], switched reluctance generator^[21].

A variable frequency-constant frequency converter (VFCF) can be used to reduce the mechanical system that leads to cost reduction in the bulky system. The converter also allows the variable frequency operation of the wind turbines in order to optimize the performance. There are a number of topologies suitable for the applications:

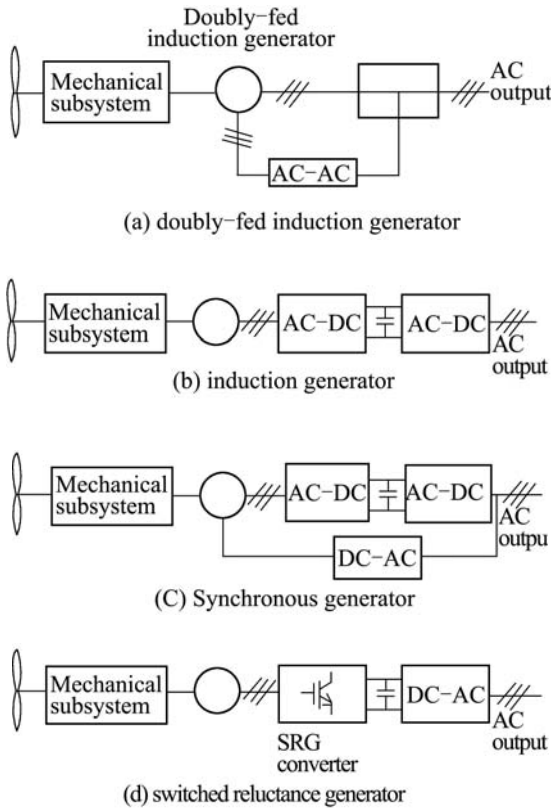


Fig. 11 Wind turbine topologies

A. AC-DC-AC converter

Basically the system is based on a cascade connection of an AC-DC and a DC-AC inverter^[22]. The intermediate stage is a DC stage which has some capacitor or even battery for intermediate energy storage and voltage smoothing. Fig.12 shows a typical schematic diagram. The capacitor C_{DC} or the battery B_{DC} can also provide a prolonged uninterrupted time in case the input stage fails to supply. The AC-DC is usually a rectifier or an AC-DC power factor correction rectifier. The DC-AC inverter is a general one.

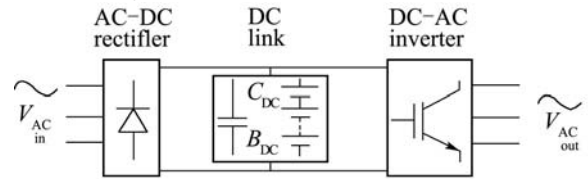


Fig. 12 AC-DC-AC converter system

B. Matrix converter

Matrix converter for AC-AC power conversion^[23] is particularly useful because of no immediate energy storage. The output voltage and frequency can be adjusted so that it is a good candidate for renewable energy generator.

C. Discussion

Both AC-DC-AC converter and the matrix converter are suitable for the VFCF application. The matrix converter uses 18 transistors but it does not require capacitors. The AC-DC-AC converter requires DC link capacitors and 6 switching devices; if the front-end AC-DC rectifier is replaced by active devices, the total amount of transistors needed is 12. The cycloconverter^[24] has a less flexibility on voltage and frequency control and is less popular.

8 Wind power tracking

The wind energy is captured by the wind turbine that converts the kinetic energy to electrical energy. The power obtained is expressed as:

$$P_r = \frac{1}{2} \rho \pi R^2 C_p(\lambda, \beta) v_w^3, \quad (15)$$

where P_r is the power received by rotor, ρ is the air density, R is the rotor blade radius, v_w is the wind speed, C_p is the power coefficient and function of tip-speed ratio λ and pitch angle β . Fig.13 shows a typical characteristic.

$$\lambda = \frac{\omega_r R}{v_w}. \quad (16)$$

The aerodynamic torque T_r is

$$T_r = \frac{1}{2} \rho \pi R^3 C_t(\lambda, \beta) v_w^2 m, \quad (17)$$

where C_t is the torque coefficient and is related to C_p as:

$$C_t(\lambda, \beta) = \lambda C_p(\lambda, \beta), \quad (18)$$

The maximum power estimation has been proposed by a number of reports. This includes using ANN, maximum power curve, maximum torque curve without knowledge of wind speed and rotor current efficiency curve.

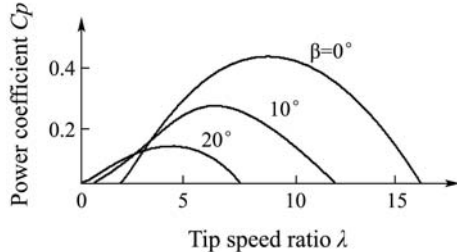


Fig. 13 Power coefficient characteristics

A. Artificial neural network(ANN)

Basically, the power equation can also be expressed as:

$$P_m = J\omega_r \frac{d\omega_r}{dt} + P_e, \quad (19)$$

where the electrical frequency ω_e and number of poles, P , is related by:

$$\omega_r = \frac{2}{P}\omega_e. \quad (20)$$

Using (19) and (20), the P_m and ω_r can be obtained from P_e and ω_e . It can then use ANN to estimate the wind speed^[25]. Fig.14 shows the control schematic.

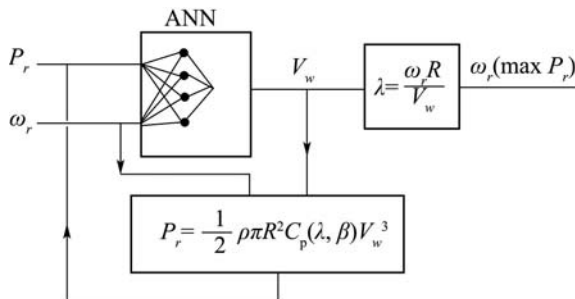


Fig. 14 ANN method for maximum power tracking

B. Power optimum curve

The characteristics of the wind turbine at various wind speeds can be shown in Fig.15. The optimum power curve by joining all the maximum points can be used for the maximum power point tracking^[21]. The optimum power curve is formed by the maximum power for different wind speeds. It can be obtained as:

$$P_{r_op} = k_{op}\omega_r^3, \quad (21)$$

where k_{op} is a constant and depends on wind turbine parameters. The generator is controlled to generate the power indicated by the maximum power curve as shown in (21) to obtain the MPT. For high wind speed, the rotor power may exceed the nominal power of the generator; pitch control can be used to reduce the received power. Fig.13 shows that β can be increased to reduce C_p .

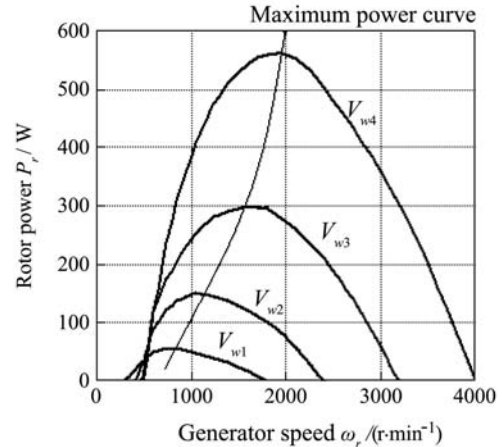


Fig. 15 A typical optimum power curve

C. Torque optimum curve

The above method requires the measurement of the wind speed. The maximum torque curve as shown in Fig.16 is equivalent to the maximum power curve as shown in Fig.15^[26]. The torque curve can be expressed as:

$$T_{r_op} = k_{top}\omega_r^2, \quad (22)$$

where k_{top} is a constant for the maximum torque curve. The generator torque is controlled according to (22) and the maximum power can be achieved.

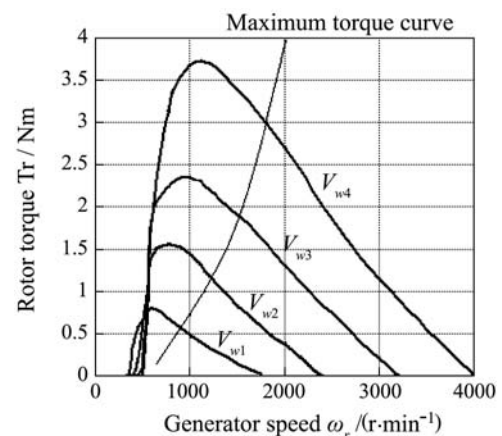


Fig. 16 A typical optimum torque curve

D. Using total power to rotor winding curve

Fig.17 shows a schematic diagram of a doubly-fed induction generator circuit. The output power P_o is re-

lated to I_r in the maximum efficient manner and the efficiency of the generator η_g is also related to I_r in a monotonic manner^[27]. The characteristic of I_r and P_o is a monotonic curve. Therefore P_o can be used to estimate I_r . The η_g can be used to estimate the received rotor power P_r . It can then be used to track the optimum wind speed and hence the rotor shaft speed.

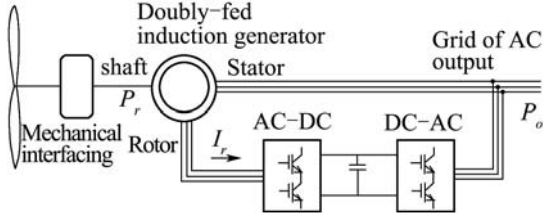


Fig. 17 The doubly-fed induction generator circuit

9 Conclusion

This paper discusses a number of topologies that can be used in alternative energy electrical system. This includes the PV array power conditioning converter, associated DC-DC converters, battery charger and inverter. The high frequency technology is used for all the power conversion units. The DC isolation is provided by the isolated DC-DC power conversion. The battery charger is designed by bi-directional circuit so that it can provide both charging and discharging capabilities. The design method is discussed. The wind power conditioning is also discussed. The MPT is examined for both solar and wind power. Power electronics gives a new era for power conversion. The power density of the power processing units is all increased. This also comes to the fact that associated materials, chassis, protection devices and control, electronics are simpler and lower in cost. With the rapid development in power devices, new topology and control method, the future power processing of alternatives energy will be more efficient and higher efficiency.

References:

- [1] KUO Y C, LIANG T J, CHEN J F. Novel maximum-power-point-tracking controller for photovoltaic energy conversion system[J]. *IEEE Trans on Industrial Electronics*, 2001, 48(3): 594 – 601.
- [2] SOLODOVNIK E V, LIU S Y, DOUGAL R A. Power controller design for maximum power tracking in solar installations[J]. *IEEE Trans on Power Electronics*, 2004, 19(5): 1295 – 1304.
- [3] SEDGHISIGARCHI K, FELIACHI A. Impact of fuel cells on load-frequency control in power distribution systems[J]. *IEEE Trans on Energy Conversion*, 2006, 21(1): 250 – 256.
- [4] CHENG K W E. *Classical Switched-mode and Resonant Power Converters*[M]. Hong Kong: The Hong Kong Polytechnic University, 2002: 78 – 80.
- [5] RODRIGUEZ C, AMARATUNGA G A J. Analytic solution to the photovoltaic maximum power point problem[J]. *IEEE Trans on Circuits and Systems—I: Fundamental Theory and Applications*, 2007, 54(9): 2054 – 2060.
- [6] TSE K K, HO M T, CHUNG H S H, et al. A novel maximum power point tracker for PV panels using switching frequency modulation[J]. *IEEE Trans on Power electronics*, 2002, 17(6): 980 – 989.
- [7] KOBAYASHI K, MATSUO H, SEKINE Y. Novel solar-cell power supply system using a multiple-input Dc-Dc converter[J]. *IEEE Trans on Industrial Electronics*, 2006, 53(1): 281 – 286.
- [8] KOBAYASHI K, MATSUO H, SEKINE Y. Sekine. An excellent operating point tracker of the solar-cell power supply system[J]. *IEEE Trans on Power Electronics*, 2006, 53(2): 495 – 499.
- [9] BLEIJS J A M, GOW J A. Fast maximum power point control of current-fed DC-DC converter for photovoltaic arrays[J]. *IEE Electronics Letters*, 2001, 37(1): 5 – 6.
- [10] MASOUM M A S, BADEJANI S M M, FUCHS E F. Microprocessor-controlled new class of optimal battery chargers for photovoltaic applications[J]. *IEEE Trans on Energy Conversion*, 2004, 19(3): 99 – 606.
- [11] AGBOSOU K, KOLHE M, HAMELIN J, et al. Performance of a stand-alone renewable energy system based on energy storage as hydrogen[J]. *IEEE Trans on Energy Conversion*, 2004, 19(3): 633 – 640.
- [12] PHAM A Q. High efficiency steam electrolyzer[S]. 2000 DOE Hydrogen Program Review, NREL/CP-570-28890.
- [13] CHENG K W E, SUTANTO D, HO Y L, et al. Exploring the power conditioning system for fuel cell[C]// IEEE PESC. Vancouver: [s.n.], 2001.
- [14] PEM fuel cell, 2004 Smithsonian Institution <http://americanhistory.si.edu/fuelcells/pemmain.htm>.
- [15] Rechargeable battery, Wikipedia Encyclopedia, Sep 2007. http://en.wikipedia.org/wiki/Rechargeable_battery.
- [16] MILLENNIUM C, EATONTOWN N J. <http://machinedesign.com/ContentItem/58345/ThechargeoftheBatteryBrigade.aspx>.
- [17] BURKE A F. Batteries and ultracapacitors for electric, hybrid, and fuel Cell Vehicles[J]. *Proc of the IEEE*, 2007, 95(4): 806 – 820.
- [18] PENA R, CLARE J C, AAHER G M. Doubly fed induction generator using back-to-back PWM converters and its application to variable-speed wind-energy generation[J]. *IEE Proceedings-EPA*, 1996, 143(3): 231 – 241.
- [19] KARRARI M, ROSEHART W, MALIK O P. Comprehensive control strategy for a variable speed cage machine wind generation unit[J]. *IEEE Trans on Energy Conversion*, 2005, 20(2): 415 – 423.
- [20] BLAABJERG F, CHEN Z, KJAER S B. Power electronics as efficient interface in dispersed power generation systems[J]. *IEEE Trans on Power Electronics*, 2004, 19(5): 1184 – 1194.
- [21] CARDENAS R, PENA R, PEREZ M, et al. Control of a switched reluctance generator for variable-speed wind energy applications[J]. *IEEE Trans on Energy Conversion*, 2005, 20(4): 781 – 791.
- [22] THOMAS R J, PHADKE AG, POTTE C. Operational characteristics of a large wind-farm utility system with a controllable AC/DC/AC interface[J]. *IEEE Trans on Power Systems*, 1988, 3(1): 220 – 225.
- [23] CHANG J, WANG A. Experimental development and evaluations of VF-input high-frequency AC–AC converter supporting distributed power generation[J]. *IEEE Trans on Power electronics*, 2004, 19(5): 1214 – 1225.
- [24] BROWN G M, SZABADOS B, HOOBLoom GJ, et al. High-power cycloconverter drive for double-fed induction motors[J]. *IEEE Trans on Industrial Electronics*, 1992, 39(3): 230 – 240.
- [25] LI H, SHI K L, MCLAREN PG. Neural-network-based sensorless maximum wind energy capture with compensated power coefficient[J]. *IEEE Trans on Industry Applications*, 2006, 41(6): 1548 – 1556.
- [26] MORIMOTO S, NAKAYAMA H, SANADA M, et al. Sensorless output maximum control for variable-speed wind generation system using IPMSG[J]. *IEEE Trans on Industry Applications*, 2005, 40(1): 60 – 67.
- [27] BHOWMIK S, SPEE R, ENSLIN J H. Performance optimization for doubly-fed wind power generation systems[J]. *IEEE Trans on Industry Applications*, 1999, 34(4): 949 – 958.